Published in final edited form as:
J Immunol. 2014 September 15; 193(6): 2812–2820. doi:10.4049/jimmunol.1401358.

Antigen signal strength during priming determines effector CD4 T cell function and antigen sensitivity during influenza virus challenge

Mika Nagaoka[,†], **Yasuko Hatta**[‡,¶], **Yoshihiro Kawaoka**[‡,§], and **Laurent P. Malherbe**[,†]

[BloodCenter of Wisconsin, Blood Research Institute, Milwaukee, WI 53226

[†]Department of Microbiology and Molecular Genetics, Medical College of Wisconsin, Milwaukee, WI

[‡]Influenza Research Institute, Department of Pathobiological Sciences, School of Veterinary Medicine, University of Wisconsin-Madison, Madison, WI 53711, USA

[§]Division of Virology, Department of Microbiology and Immunology, University of Tokyo, Tokyo 108-8639, Japan

[¶]FluGen, Inc. 597 Science Drive, Madison, WI 53711, USA

Abstract

TCR signal strength during priming is a key determinant of CD4 T cell activation but its impact on effector CD4 T functions *in vivo* remains unclear. In this study, we compare the functionality of CD4 T cell responses induced by peptides displaying varying binding half-lives with MHC class II before and after influenza virus infection. While significant quantitative and qualitative differences in CD4 T cell responses were observed before infection between mice vaccinated with low or high stability peptides, both mice mounted robust early Th1 effector cytokine responses upon influenza challenge. However, only effector CD4 T cells induced by low stability peptides proliferated and produced IL-17A after influenza challenge. In contrast, effector T cells elicited by higher stability peptides displayed a terminally differentiated phenotype and divided poorly. This defective proliferation was T cell-intrinsic but could not be attributed to a reduced expression of lymph node homing receptors. Instead, we found that CD4 T cells stimulated with higher stability peptides exhibited decreased responsiveness to low levels of Ag presentation. Our study reveals the critical role of TCR signal strength during priming for the function and Ag sensitivity of effector CD4 T cells during viral challenge.

Introduction

Th1 cells produce IFN-γ and mediate protective immunity against intracellular pathogens. In contrast to the remarkable homogeneity of *in vitro*-induced Th1 cells, Th1 cells induced by vaccines and pathogens *in vivo* are phenotypically and functionally heterogeneous. Although it is known that Th1 cell quality rather than quantity plays an important role in their efficacy

Correspondence should be addressed to: aurent P. Malherbe, BloodCenter of Wisconsin, Blood Research Institute, P.O. Box 2178, Milwaukee, WI, 53201, Phone: (414) 937-6829, Fax: (414) 937-6284, laurent.malherbe@bcw.edu.

in vivo (1), the parameters controlling the robustness of CD4 T cell responses during pathogen challenge remain poorly defined.

The strength of TCR interaction with peptides bound to MHC class II molecules (pMHCII) is central to CD4 T cell proliferation and differentiation (2). In general, strong TCR signals favor the differentiation of Th1 cells (3, 4), suggesting that increasing TCR signal strength during priming would improve the quality and efficiency of cellular immunity (5, 6). However, experiments in murine experimental autoimmune encephalomyelitis model have suggested that strong TCR stimulation decreased effector CD4 T cell encephalitogenicity (7). How TCR signal strength during priming changes effector CD4 T cell functions is therefore still unclear.

We have previously shown using peptides mutated at MHCII anchor residues that pMHCII stability regulates the magnitude, quality and clonotypic diversity of the effector CD4 T cell compartment (8, 9). In the current studies, we used a recombinant influenza virus to analyze the impact of pMHCII stability on effector CD4 T cell function during viral challenge. We found that effector CD4 T cells induced by lower stability peptides proliferated rapidly in response to influenza virus challenge and exhibited significant plasticity in their cytokine production. In contrast, effector CD4 T cells induced by higher stability peptides displayed a terminally differentiated phenotype and proliferated poorly after virus challenge. This defective proliferative response could be attributed to a decrease in Ag sensitivity. Taken together, our results reveal the importance of TCR signal strength during priming for effector CD4 T cell responses during viral challenge.

Materials and Methods

Mice

B10.BR, B10.BR-Thy1.1 congenic, and 5C.C7αβ transgenic mice have been described before (9) Mice were maintained under pathogen-free conditions at The Medical College of Wisconsin. The Medical College of Wisconsin and the Institutional Animal Care and Use Committee reviewed and approved all experiments.

Peptide synthesis

$PCC_{88–104}$ (KAERADLIAYLKQATAK), PCC_{103K} (KAERADLIAYLKQATKK), and $MCC_{88–103}$ (ANERADLIAYLKQATK) peptides were synthesized by standard solid-phase methods, purified by HPLC, and confirmed by mass spectrometry as previously described (9). Hemoglobin peptide ($Hb_{64–76}$) was purchased from AnaSpec (San Jose, CA).

Immunization and adoptive transfer

Mice were immunized s.c. at the base of the tail with 60 μg of peptide in combination with monophosphoryl lipid A (MPL)-based adjuvant [laboratory formulation based on procedures in (10)]. For adoptive transfer, 2.5×10^5 total splenocytes from 5C.C7αβ transgenic mice containing 4×10^4 naive PCC-specific CD4 T cells were transferred i.v. into B10.BR-Thy1.1 congenic mice at the time of immunization.

Generation of Recombinant WSN-MCC$_{88–103}$ Virus

To generate the recombinant WSN mutant virus (WSN-MCC$_{88–103}$), we inserted the oligonucleotidic sequence encoding MCC$_{88–103}$ (5’-GCAAACGAACGTGCAGATCTCATCGCCTATCTAAAACAAGCTACTAAG-3’) between nucleotides 145 and 146 of WSN NA gene. Insertion of up to 28 aa into the NA stalk does not impair NA function but insertion of more than 12 aa attenuates the virus. A/WSN/33 (WSN; H1N1) and WSN-MCC was generated by using plasmid-based reverse genetics (11). Viruses were amplified and plaqued on Madin-Darby Canine Kidney (MDCK) cells.

Influenza infection

Mice were i.p. injected with 100 μl of a combination of xylazine (2 mg/ml) and ketamine (15 mg/ml) (Midwest Veterinary Supply) in PBS. Mice were infected intranasally under anesthesia with 2400 PFU recombinant WSN-MCC$_{88–103}$ virus in 30 μl of PBS. All infected mice were housed in the biocontainment suite at the animal facility of the Medical College of Wisconsin where tissue harvest from infected mice was also performed.

Quantitation of viral RNA by qPCR

Viral RNA was detected in a manner similar to previously published protocols (12, 13). RNA was isolated from lung homogenates using TRIzol (Sigma-Aldrich) and RNA was reverse-transcribed into cDNA using a gene specific primer targeted to influenza acid polymerase (PA) negative sense RNA (PA RT 5’-GTGCGACAATGCTTCAATCC-3’) and Superscript II reverse transcriptase (Invitrogen Life Technologies). cDNA was then used for amplification by quantitative real-time PCR (iCycler; Biorad) using primers specific for influenza PA gene (PA forward 5’-CGGTCCAAATTCCTGCTGA-3’, PA reverse 5’-CATTGGGTTCCTTCCATCCA-3’). The negative control consisted of lung homogenates from uninfected naïve B10.BR mice. The PA-gene copy number was calculated from a known concentration of PA-containing plasmid (a gift from Dr. R Webster, St. Jude Children’s Research Hospital, Memphis, TN) used as a standard curve in all reactions. PA copies per lung were then calculated based on the total amount of RNA in each lung sample.

Preparation of single cell suspensions from organs

At the indicated times, mice were euthanized by CO_2 inhalation followed by exsanguination by perforation of the abdominal aorta. Lungs were perfused by injecting 3 ml of PBS in the left ventricle of the heart. Cells in the lung airways were harvested after intratracheal introduction and recovery of 1 mL PBS three times. Single cells were prepared from draining lymph nodes (LNs) and spleen as described previously (9). Preparation of lung single-cell suspensions after enzymatic digestion was described elsewhere (14). Briefly, lungs were removed, minced, and incubated in digest media containing 250 U/ml collagenase type 1 (Worthington, Lakewood, NJ), 5 U/ml hyaluronidase (Sigma-Aldrich, St. Louis, MO), and 50 U/ml DNase I (Worthington) for 1 h at 37°C, and 2 mM EDTA was added for the last 15 min. The single-cell suspension was filtered through 40-μm pore cell strainers after removing erythrocytes by NH_4Cl hypotonic lysis buffer.

For the analysis of dendritic cell (DC) population, draining LNs were harvested, cut into small fragments, and digested with 2 mg/ml collagenase D (Roche, Mannheim, Germany) and 50 U/ml DNase I (Worthington) in HBSS with calcium and magnesium for 30min at 37°C, followed by the addition of 10 mM EDTA for a further 5 min.

BrdU labeling *in vivo*

Twenty-four hour before sacrificed, mice were i.p. injected with 1 mg of BrdU (BD Biosciences, San Jose, CA). BrdU incorporation was assessed using a BrdU Flow kit (BD Biosciences) according to the manufacturer's instructions.

Measurement of Cytokines

Bronchoalveolar lavage fluid (BALF) was obtained by flushing the airway with 1 ml sterile PBS. We spun down the cells and collected supernatants. The level of cytokines in the supernatants was measured with the BioRad multiplex assay (BioRad Laboratories, Hercules, CA) in accordance with the manufacturer's instructions.

Flow cytometry

Cell suspensions were labeled for 45 min at 4°C at a density of 2×10^8 cells/ml with predetermined optimal concentrations of the following fluorophore-labeled mAbs: FITC-conjugated anti-Va11 (RR8.1), anti-I-Ek (14.4.4), PE or biotin-conjugated anti-Vb3 (KJ25; all produced in the laboratory); Pacific Blue-conjugated anti-CD3 (17A2), anti-CD19 (6D5), PE-conjugated anti-CD49a (HMa1), anti-CD80 (16-10A1), anti-CCR7 (4B12), APC-conjugated anti-KLRG1 (2F1/KLRG1), anti-CXCR3 (CXCR3-173), anti-CD62L (MEL-14), FITC or APC/Cy7-conjugated anti-Thy1.1 (OX-7), anti-Thy1.2 (30-H12), APC/Cy7-conjugated anti-CD44 (IM7), anti-CD11c, biotin-conjugated anti-CD69 (H1.2F3; all from Biolegend, San Diego, CA); PerCP/Cy5.5-conjugated Streptavidin, biotin-conjugated anti-CD103 (2E7), eFluor450-conjugated anti-CD11b (M1/70), anti-CD8a (53-6.7), anti-B220 (RA3-6B2; all from eBioscience, San Diego, CA); Purified rat anti-mouse CD16/CD32 antibody (clone 93, produced in the laboratory) was used to prevent nonspecific binding of antibodies to the Fc receptors. After staining, cells were suspended in 1.5 μg/ml DAPI (Life Technologies, Carlsbad, CA) for dead cells exclusion.

Apoptosis was determined with the FLICA Kit (Life Technologies) according to the manufacturer's protocol.

For intracellular staining, cells were stained with Fixable Viability Stain 450 (BD Biosciences, San Jose, CA) following surface staining. Cells were fixed and permeabilized using BD Cytofix/CytopermTM (BD Biosciences). Intracellular proteins were stained for 30 min at RT with FITC-conjugated anti-Ki67 (B56, BD Biosciences) according to the manufacturer's protocol.

Data were collected with FACS Diva software (BD Biosciences) and were analyzed with FlowJo software (Tree Star, Ashland, OR). Profiles are presented as 5% probability contours with outliers.

Ex vivo restimulation and intracellular cytokine staining

Cell suspensions in RPMI 1640 supplemented with 10% FCS, 50 nM 2-ME were plated in 24-well plates (10^7 cells/mL) and restimulated with 20 ng/ml PMA and 1 μg/ml ionomycin for 4 h. Stimulated cells were resuspended in anti-CD16/32 antibody (produced in the laboratory) in PBS with 5% FCS and labeled for surface markers and dead cells as described above. Cells were fixed using BD Cytofix/Cytoperm™ (BD Biosciences). PE-labeled anti-IL-17A (TC11-18H10.1), and APC-labeled anti-IFN-γ (XMG1.2) antibodies (all Biolegend) were diluted in Perm/Wash Buffer (BD Biosciences) and incubated with fixed cells for 30 min at room temperature. Cells were washed with Perm/Wash Buffer followed by PBS with 5% FCS and analyzed.

In vivo Proliferation assay

Vaccine-primed $CD4^+$ T cells were enriched from draining LN and spleen by Dynal negative selection (Life Technologies). $Thy1.2^+$ 5C.C7 cells were sorted on a BD Aria by removing $Thy1.1^+$ cells. B10.BR-Thy1.1 mice were infected with WSN-$MCC_{88–103}$ virus following adoptive transfer of $2×10^5$ sorted 5C.C7 cells. BrdU was i.p. injected 24 h before analysis as described above.

Ex vivo proliferation assay

Single cell suspensions from draining LN and spleens from immunized mice were negatively selected for CD4 T cells using Streptavidin RapidSphere EasySep (StemCell Technologies, Vancouver, CA), biotin-conjugated anti-CD8a (53-6.7) and anti-B220 (RA3-6B2, all Biolegend). $Thy1.2^+$ 5C.C7 cells were sorted on a BD Aria. Sorted 5C.C7 cells were labeled with 5 μM CFSE using labeling procedure described previously(15). $CD11c^+$ cells were purified by positive selection (Miltenyi Biotec, Auburn, CA) from spleens of naïve mice or mediastinal LNs (MLNs) of the mice infected with WSN-$MCC_{88–103}$ virus 2 days before. $CD103^+CD11b^-$ or $CD103^-CD11b^+$ DCs in MLN were sorted on Aria.

$2×10^4$ CFSE-labeled 5C.C7 cells were co-cultured with $2–4×10^3$ splenic DCs or MLN DCs at the indicated concentrations of $MCC_{88–103}$ peptide in 96-well plate, and proliferation was measured as CFSE dilution after 3 days.

Statistical analysis

Statistical differences between experimental groups were determined by the Student t test. Correlations between parameters were assessed by the Spearman correlation analysis. Statistical analysis was conducted with Prism software (GraphPad Software, La Jolla, CA). $p < 0.05$ was considered statistically significant.

Results

Strong TCR signals alter the magnitude and quality of CD4 T cell response induced by TLR4 agonists

We have previously performed peptide dissociation assay with soluble I-E^k molecules to determine pMHCII half-lives and shown that $PCC_{88–104}$ peptides form low stability

pMHCII (t1/2 = 5 h) that were 50-fold less stable than pMHCII formed by its higher stability variant PCC_{103K} (t1/2 = 229 h). To examine the impact of TCR signal strength on the magnitude and quality of Th response, we immunized B10.BR mice subcutaneously with $PCC_{88–104}$ or PCC_{103K} in an adjuvant system based on the TLR4 agonist MPL (8). After 7 days, polyclonal Ag-specific Th cells in draining LN, spleen and lung were analyzed. Immunization with high stability peptide PCC_{103K} increased the total number of Ag-specific Th cells in all organs examined (Fig. 1 A). When restimulated *in vitro*, significantly higher number of IFN-γ^+ Th1 cells were detected in the cells primed with high stability peptides (Fig. 1 B&C) while few cells produced IL-17 (Fig. 1 B&D). Immunization with high stability peptides not only enhanced Th1 cell differentiation but also induced a number of phenotypic changes in Th1 cells (M. Nagaoka, C.K. Baumgartner, and L.P. Malherbe, submitted for publication), the most dramatic being the upregulation of CD49a (VLA-1), an alpha subunit of $\alpha1\beta1$ integrin that has been shown to play an important role in T cell responses during influenza virus infection (16, 17) (Fig. 1 E&F). Overall, strong TCR signal during priming not only increased the magnitude of Th1 response but also changed Th1 cell quality.

Effector Th1 cells induced by TLR4 agonists are rapidly mobilized in response to influenza challenge

To assess *in vivo* effector functions of Th cells primed with different TCR signal strength, we created a recombinant influenza A virus carrying moth cytochrome c peptide epitope (WSN-$MCC_{88–103}$), a peptide that form intermediate stability pMHCII with I-E^k (t1/2 = 73 h) (8). This peptide was chosen because $PCC_{88–104}$ is known to raise a heteroclitic response to $MCC_{88–103}$, which means that all T cell clones raised by immunization with $PCC_{88–104}$ respond better to $MCC_{88–103}$ (18). Infection of B10.BR mice with WSN-$MCC_{88–103}$, unlike WT WSN, induced the expansion of cytochrome c-specific $V\alpha11^+V\beta3^+CD44^{hi}CD62L^{lo}$ cells (8, 19), confirming that the cytochrome c peptide is presented during infection (data not shown). Unlike mice immunized with control I-E^k binding hemoglobin peptide ($Hb_{64–76}$), mice immunized with $PCC_{88–104}$ or PCC_{103K} displayed a rapid accumulation of Ag-specific Th cells in the BAL and lung (Fig. 2 A) 4 days after challenge with WSN-$MCC_{88–103}$ virus. Although high stability peptides induced higher number of Th1 cells in secondary lymphoid organs before infection (Fig. 1 B), a comparable number of Ag-specific Th1 cells were found in the infected lung 4 days after virus challenge in mice immunized with high or low stability peptide-immunized mice (Fig. 2 B). Furthermore, similar elevated levels of Th1-associated cytokines (IFN-γ and IL-2) and low levels of anti-inflammatory cytokines (IL-10) were detected in the BALF of these mice (Fig. 2 C). These data suggest that, irrespective of TCR signal strength during priming, vaccine-induced Th1 cells were rapidly recruited to the lung and produced effector cytokines upon viral infection.

Plasticity of effector CD4 T cells induced by weaker TCR signals

We have shown that few Ag-specific Th17 cells were elicited following immunization with low or high stability peptides (Fig. 1 C). Surprisingly, we found that IL-17 level in the BALF on day 4 postinfection was significantly higher in mice immunized with low stability peptides (Fig. 3 A). Intracellular cytokine staining confirmed that only Th cells primed with low stability peptides produced IL-17 in infected lungs (Fig. 3 B&C). Furthermore, about

40% of IL-17$^+$ cells coproduced IFN-γ (Fig. 3 B&C). IL-17$^+$IFN-γ$^+$ cells were not detected in any organs (LN, Spleen, lung) prior to challenge (Fig. 1 C) suggesting that effector CD4 T cells induced by weaker TCR signal maintained functional plasticity during influenza challenge.

Defective proliferative response impaired accumulation of strongly stimulated effector CD4 T cells following influenza challenge

Previous studies have shown that temporally distinct waves of effector cells are necessary to mediate a sustained response to influenza virus infection (20). When we analyzed Th cell responses at a later stage of infection (day 6 postinfection), we found that Ag-specific Th cells primed with low stability peptides continued to accumulate in the lung between day 4 and day 6 postinfection exceeding the number of Th cells induced with high stability peptides (Fig. 4 A). We have previously shown by single-cell repertoire analysis that low stability peptides promote the selective expansion of high avidity T cells while higher stability peptides expand lower avidity clonotypes (8). It was therefore possible that high and low avidity clonotypes differed in their capacity to accumulate during viral challenge. To investigate this possibility, we adoptively transferred cytochrome c-specific monoclonal 5C.C7 TCR transgenic T cells to congenic recipients before peptide immunization and tracked their accumulation in response to virus challenge. Consistent with our observations in the polyclonal response, we found that 5C.C7 cells primed with higher stability peptides were present in high number in the lung prior to virus challenge (Fig. 4 B) but their number remained constant during the first six days of infection. In contrast, the number of 5C.C7 cells primed with low stability peptides increased 16-fold during the same timespan (Fig. 4 B). Therefore, independently of TCR usage, immunization with lower stability peptides promoted a superior accumulation of Ag-specific CD4 T cells later after influenza challenge.

The difference in effector T cell accumulation between mice primed with low and high stability peptides could reflect a difference in apoptosis or proliferation. No difference in the number of apoptotic 5C.C7 T cells at day 4 postinfection was observed between recipients immunized with high or low stability peptides (data not shown). In contrast, 5C.C7 T cells primed with high stability peptides expressed significantly higher levels of KLRG1, a marker associated with terminally differentiated cells with poor proliferative capacity (21) (Fig. 5 A). Accordingly, less pulmonary Ag-specific CD4 T cells expressed Ki67 (Fig. 5 B) or incorporated BrdU (Fig. 5 C) on day 4 after influenza challenge in mice immunized with high stability peptides, suggesting a defective proliferation was responsible for the poor accumulation of effector CD4 T cells in these mice.

Lung-derived DCs in MLNs play a critical role in initiating T cell proliferative response following primary and secondary influenza infections (20, 22). We found that BrdU incorporation (Fig. 5 D), Ki67 expression (Fig. 5 E), and CD69 expression (Fig. 5 F) at day 4 postinfection were also significantly reduced in high stability peptide-primed Th cells present in MLN. Overall, these data suggest that Th cells primed with strong TCR signals have decreased proliferative capacity in response to viral infection.

The proliferative defect in mice primed with strong TCR signal is CD4 T cell intrinsic

The defective proliferative response in mice primed with high stability peptides can be mediated by T-cell intrinsic or extrinsic mechanisms. One of the phenotypic changes observed in a fraction of Th cells primed with higher stability peptides is the acquisition of granzyme B (M. Nagaoka, C.K. Baumgartner, and L.P. Malherbe, submitted for publication). Cytotoxic CD4 T cells could affect early Ag presentation by decreasing viral titer in the lungs (13) or by killing Ag-presenting APCs (23). To determine whether priming CD4 T cells with higher stability peptides had an impact on early viral replication in the lung, a quantitative PCR-based assay that detects the influenza A PA gene copy number was used (24). Fig. 6A shows PA gene copy number per lung at day 4 postinfection and demonstrates that the lungs of mice immunized with low or high stability peptides contained significantly less viral RNAs than the lungs of mice immunized with control hemoglobin peptides, suggesting that effector CD4 T cells impacted early viral replication but cytotoxic CD4 T cells. However, comparable amount of viral RNAs were found following immunization with low or high stability peptides.

Airway-resident $CD103^+$ DCs play a critical role in Ag presentation to T cells in MLN following influenza infection (25). To determine whether CD4 T cells primed with higher stability peptides impacted Ag-presenting DCs in MLN, we analyzed DCs in MLN 2 days after challenge. The numbers of total DCs or $CD103^+$ DCs in MLN (Fig. 6 B&C), as well as their expression levels of MHCII and CD80 (Fig. 6D) were comparable between mice immunized with high or low stability peptides, suggesting that cytotoxic CD4 T cells induced by high stability peptides did not alter Ag presentation following virus challenge.

To further determine whether the defect in T cell proliferation was T-cell intrinsic or extrinsic, we primed 5C.C7 T cells with low stability peptides *in vivo*, transferred them into secondary recipients previously immunized with low or high stability peptides, and monitored their proliferative response following influenza challenge. No difference in BrdU incorporation was observed between 5C.C7 effector cells transferred in recipients immunized with low or high stability peptides on day 4 postinfection (Fig. 6 E). In contrast, when we transferred peptide-primed 5C.C7 effector T cells into secondary recipients previously immunized with low stability peptides, we found that effector cells primed with higher stability peptides exhibited a significantly reduced capacity to proliferate in response to viral challenge (Fig. 6 F). Therefore, these data imply that T cell–intrinsic mechanisms control CD4 T cell proliferative response following influenza challenge.

Strong TCR signals During Priming Increase Ag Threshold Requirement for Recall proliferation

The expression of LN homing receptors CD62L and CCR7 distinguishes Ag-specific CD4 T cell subsets with high proliferative capacity (26–28). CCR7 has also been shown to regulate CD4 T cell migration from tissues into draining LNs (29, 30). Therefore, we examined CD62L and CCR7 expression on Ag-specific CD4 T cells after immunization. We found that a similar frequency of 5C.C7 cells expressed CD62L following immunization with low or high stability peptides but less 5C.C7 cells expressed CCR7 in the draining LNs of mice immunized with high stability peptides (Fig. 7 A&B). However, the total numbers of Ag-

specific CD4 T cells in MLNs at early stage of infection (day 2 postinfection) were comparable between mice immunized with high or low stability peptides (data not shown), suggesting that Th cells primed with strong TCR signal were recruited to MLNs during virus challenge.

Next, we assessed the proliferative response of Th cells to lung-derived DCs. $CD103^+$ or $CD103^-$ DCs in MLNs at day 2 postinfection were sorted and co-cultured for 3 days with CFSE-labeled 5C.C7 cells primed with high or low stability peptides. Regardless of lung DC subset, dramatic differences in effector T cell division were observed. Whereas over 20–30% of effector T cells stimulated with low stability peptides had divided within 3 days, only 5% of the effector T cells stimulated with high stability peptides had entered cell cycle (Fig. 7C). Interestingly, when 1μM of cognate peptides were added to lung DCs, 5C.C7 cells induced by high stability peptides proliferated comparable to or better than cells induced by low stability peptides (Fig. 7 D), suggesting that strongly stimulated CD4 T cells divide poorly *in vivo* in response to low doses of Ag. To further characterize the impact of peptide stability on the Ag sensitivity of effector CD4 T cells, CFSE-labeled 5C.C7 cells primed with high or low stability peptides were stimulated with purified splenic DCs from naïve mice in the presence of various concentrations of peptides. We found that 5C.C7 cells primed with low stability peptides proliferated preferentially at low peptide concentrations (from 1 pM to 10 nM) while high stability peptide-primed 5C.C7 cells proliferated better at high Ag concentrations (from 10 nM to 1 μM) (Fig. 7 E&F).

Modulating surface TCR expression is the best known mechanism for tuning T-cell Ag sensitivity. To determine if the distribution of the 5C.C7 TCR was similar in effector 5C.C7 cells stimulated with low or high stability peptides, we stained for cell surface expression of the transgenic Vα11 and Vβ3 TCR chains. We found that Vα11 expression was reduced in 5C.C7 cells stimulated with high stability peptides (Fig. 7G). However, no reduction in Vβ3 expression was observed (data not shown) and the reduction in Vα11 expression was not observed in the spleen (Fig. 7G). When we compared the Ag sensitivity of 5C.C7 cells derived from draining LN and spleen, we found that, irrespective of their organs of origin, cells primed with low stability peptides proliferate better at low Ag dose (Fig. 7H). Therefore, we concluded that TCR signal strength during priming tunes Ag sensitivity independently of TCR expression level.

Discussion

Our studies reveal the remarkable impact of TCR signal strength during priming on effector CD4 T cell functions in response to viral infection. Although mice primed with low or high stability peptides mounted comparable Th1 responses early after influenza challenge, their effector CD4 cells differ in their plasticity and Ag sensitivity. Effector CD4 T cells induced by lower stability peptides quickly proliferated upon influenza challenge and simultaneously initiated IL-17 production. In contrast, effector CD4 T cells induced by high stability peptides did not secrete IL-17, developed a terminally differentiated phenotype, and proliferated poorly in response to viral infection. This defective proliferation was T-cell intrinsic and caused by a decreased sensitivity to low-density Ag presentation.

T cell sensitivity to Ag stimulation has long been known to be regulated by T cell activation status. *In vitro* derived effector (31, 32) and memory (33, 34) CD4 T cells have been shown to display enhanced proliferation in response to low Ag dose. The increased sensitivity of Ag-experienced T Cells has been attributed to an increased in the size of oligomeric TCR complexes (35) and a superior calcium mobilization and phosphorylation of signaling molecules downstream of the TCR (31). Interestingly, in several studies, low stability $PCC_{88–104}$ peptides were used to analyze effector/memory CD4 T cell responsiveness to Ag stimulation (31, 32, 34). Our studies demonstrate that the stability of the priming peptides plays a critical role in the sensitivity of the resulting effector CD4 T cells. Ag-specific CD4 T cells induced by higher stability peptides *in vivo* were less sensitive than CD4 T cells elicited by low stability peptides and than naïve CD4 T cells themselves. Our results may also explain why in murine experimental autoimmune encephalomyelitis model, Th cells induced by higher stability peptides did not accumulate in the central nervous system and failed to induce disease (7, 36).

Several studies have shown that the Ag sensitivity of naïve T cells is constantly tuned by basal TCR signals derived from self-pMHCII recognition on DCs by a poorly understood mechanism (37–39). Whether effector CD4 T cells still perceive this tonic TCR signal is unclear but it is known that memory CD4 T cells are less dependent upon MHC class II-derived signals than naïve CD4 T cells for their homeostasis (40).

Our studies reveal the functional importance of TCR signaling strength during priming for effector CD4 T cell proliferation in response to influenza virus challenge. Effector CD4 T cells induced by strong TCR signals were defective in initiating proliferation and accumulating in response to viral challenge. Interestingly, influenza-virus specific memory CD8 T cells have also been shown to differ in their capacity to mount a proliferative response upon virus challenge. As suggested in our studies, CD62L expression on T cells was not predictive of their proliferative capacity (41). Instead, for both CD4 T cells (our results) and CD8 T cells (42, 43) the limiting factor appears to be their capacity to proliferate in response to limited Ag concentration present on the surface of lung-derived DCs in MLN following influenza challenge. Hence, tissue-derived DCs during viral infection may set the Ag threshold for recall proliferation (44) and select effector/memory T cells based on the strength of their past Ag stimulation.

Our studies highlight another important role of TCR signaling strength during priming for effector CD4 T cell response to influenza virus infection. While strongly stimulated CD4 T cells developed a terminally differentiated phenotype in response to viral infection, CD4 T cells stimulated with weaker peptides increased their production of IL-17A. While some IL-17A-producing cells were detected prior to virus challenge, none of them co-produced IFN-γ and their numbers were not significantly different between mice primed with low or high stability peptides. Woodworth et al. have recently reported similar functional differences between CD4 T cells elicited by dominant or cryptic epitopes upon challenge with *Mycobacterium tuberculosis* (45). Dominant epitope-specific CD4 T cells become terminally differentiated upon bacterial challenge while cryptic epitope-specific T cells enhanced IL-17A production. These results suggest that effector Th1 cells elicited by suboptimal TCR stimulation (lower stability peptides, cryptic epitopes) exhibit considerable

plasticity for future IL-17 expression (46–48), perhaps due decreased exposure to Th1 polarizing cytokines (49).

In summary, our data reveal the critical role of TCR signal strength during priming for the plasticity and Ag sensitivity of effector CD4 T cells during virus challenge. These findings could have important implications in the design of new vaccination approaches to protect against pathogens.

Acknowledgments

We would like to thank Drs Stacey Schultz-Cherry, Subramaniam Malarkannan and Hailong Guo for assistance with virus preparation and Drs Dorothy Cheung and Mitchell Grayson for help with viral infection.

This work was supported, in part by grant 1UL1RR031973 from the Clinical and Translational Science Award (CTSI) program of the National Center for Research Resources (LPM), the American Cancer Society (LPM), the Medical College of Wisconsin Cancer (LPM), and National Institute of Allergy and Infectious Diseases Public Health Service research grants (YK). YK was also supported by the Strategic Basic Research Programs of Japan Science and Technology Agency.

Abbreviations used in this paper

BALF	bronchoalveolar lavage fluid
DC	dendritic cell
LN	lymph node
MLN	mediastinal lymph node
MCC	moth cytochrome c
MFI	mean fluorescence intensity
MPL	monophosphoryl lipid A
PCC	pigeon cytochrome c
pMHCII	peptide-MHC class II
ICS	intracellular cytokine staining

References

1. Seder RA, Darrah PA, Roederer M. T-cell quality in memory and protection: implications for vaccine design. Nature Reviews Immunology. 2008; 8(4):247–258.
2. Corse E, Gottschalk RA, Allison JP. Strength of TCR-Peptide/MHC Interactions and In Vivo T Cell Responses. Journal of Immunology. 2011; 186(9):5039–5045.
3. Constant SL, Bottomly K. Induction of Th1 and Th2 CD4+ T cell responses: the alternative approaches. Annual review of immunology. 1997; 15:297–322.
4. Kim C, Wilson T, Fischer KF, Williams MA. Sustained Interactions between T Cell Receptors and Antigens Promote the Differentiation of CD4(+) Memory T Cells. Immunity. 2013; 39(3):508–520. [PubMed: 24054329]
5. Ahlers JD, Belyakov IM, Thomas EK, Berzofsky JA. High-affinity T helper epitope induces complementary helper and APC polarization, increased CTL, and protection against viral infection. Journal of Clinical Investigation. 2001; 108(11):1677–1685. [PubMed: 11733563]
6. Berzofsky JA, Ahlers JD, Belyakov IM. Strategies for designing and optimizing new generation vaccines. Nature Reviews Immunology. 2001; 1(3):209–219.

7. Minguela A, Pastor S, Mi WT, Richardson JA, Ward ES. Feedback regulation of murine autoimmunity via dominant anti-inflammatory effects of interferon gamma. Journal of Immunology. 2007; 178(1):134–144.
8. Baumgartner CK, Ferrante A, Nagaoka M, Gorski J, Malherbe LP. Peptide-MHC Class II Complex Stability Governs CD4 T Cell Clonal Selection. Journal of Immunology. 2010; 184(2):573–581. PMCID: PMC2975033.
9. Baumgartner CK, Yagita H, Malherbe LP. A TCR Affinity Threshold Regulates Memory CD4 T Cell Differentiation following Vaccination. Journal of Immunology. 2012; 189(5):2309–2317. PMCID: PMC3424363.
10. Baldridge JR, Crane RT. Monophosphoryl lipid A (MPL) formulations for the next generation of vaccines. Methods. 1999; 19(1):103–107. [PubMed: 10525445]
11. Neumann G, Watanabe T, Ito H, Watanabe S, Goto H, Gao P, et al. Generation of influenza A viruses entirely from cloned cDNAs. Proceedings of the National Academy of Sciences of the United States of America. 1999; 96(16):9345–9350. [PubMed: 10430945]
12. Vester D, Lagoda A, Hoffmann D, Seitz C, Heldt S, Bettenbrock K, et al. Real-time RT-qPCR assay for the analysis of human influenza A virus transcription and replication dynamics. Journal of virological methods. 2010; 168(1–2):63–71. [PubMed: 20433869]
13. Brown DM, Dilzer AM, Meents DL, Swain SL. CD4 T cell-mediated protection from lethal influenza: Perforin and antibody-mediated mechanisms a one-two punch. Journal of Immunology. 2006; 177(5):2888–2898.
14. Cheung DS, Ehlenbach SJ, Kitchens RT, Riley DA, Thomas LL, Holtzman MJ, et al. Cutting Edge: CD49d(+) Neutrophils Induce Fc epsilon RI Expression on Lung Dendritic Cells in a Mouse Model of Postviral Asthma. Journal of Immunology. 2010; 185(9):4983–4987.
15. Quah BJC, Parish CR. New and improved methods for measuring lymphocyte proliferation in vitro and in vivo using CFSE-like fluorescent dyes. Journal of Immunological Methods. 2012; 379(1–2):1–14. [PubMed: 22370428]
16. Ray SJ, Franki SN, Pierce RH, Dimitrova S, Koteliansky V, Sprague AG, et al. The collagen binding alpha 1 beta 1 integrin VLA-1 regulates CD8 T cell-mediated immune protection against heterologous influenza infection. Immunity. 2004; 20(2):167–179. [PubMed: 14975239]
17. Chapman TJ, Topham DJ. Identification of a Unique Population of Tissue-Memory CD4(+) T Cells in the Airways after Influenza Infection That Is Dependent on the Integrin VLA-1. Journal of Immunology. 2010; 184(7):3841–3849.
18. Solinger AM, Ultee ME, Margoliash E, Schwartz RH. T-lymphocyte response to cytochrome c. I. Demonstration of a T-cell heteroclitic proliferative response and identification of a topographic antigenic determinant on pigeon cytochrome c whose immune recognition requires two complementing major histocompatibility complex-linked immune response genes. Journal of Experimental Medicine. 1979; 150(4):830–848. [PubMed: 92520]
19. McHeyzer-Williams LJ, Panus JF, Mikszta JA, McHeyzer-Williams MG. Evolution of antigen-specific T cell receptors in vivo: Preimmune and antigen-driven selection of preferred complementarity-determining region 3 (CDR3) motifs. Journal of Experimental Medicine. 1999; 189(11):1823–1837. [PubMed: 10359586]
20. Hikono H, Kohlmeier JE, Ely KH, Scott I, Roberts AD, Blackman MA, et al. T-cell memory and recall responses to respiratory virus infections. Immunological Reviews. 2006; 211:119–132. [PubMed: 16824122]
21. Reiley WW, Shafiani S, Wittmer ST, Tucker-Heard G, Moon JJ, Jenkins MK, et al. Distinct functions of antigen-specific CD4 T cells during murine Mycobacterium tuberculosis infection. Proceedings of the National Academy of Sciences of the United States of America. 2010; 107(45): 19408–19413. [PubMed: 20962277]
22. Braciale TJ, Sun J, Kim TS. Regulating the adaptive immune response to respiratory virus infection. Nature Reviews Immunology. 2012; 12(4):295–305.
23. van de Berg PJ, van Leeuwen EM, Ten Berge IJ, van Lier R. Cytotoxic human CD4(+) T cells. Current Opinion in Immunology. 2008; 20(3):339–343. [PubMed: 18440213]

24. van Elden LJ, Nijhuis M, Schipper P, Schuurman R, van Loon AM. Simultaneous detection of influenza viruses A and B using real-time quantitative PCR. J Clin Microbiol. 2001; 39(1):196–200. PMCID: 87701. [PubMed: 11136770]
25. Neyt K, Lambrecht BN. The role of lung dendritic cell subsets in immunity to respiratory viruses. Immunological Reviews. 2013; 255(1):57–67. [PubMed: 23947347]
26. Sallusto F, Lenig D, Forster R, Lipp M, Lanzavecchia A. Two subsets of memory T lymphocytes with distinct homing potentials and effector functions. Nature. 1999; 401(6754):708–712. [PubMed: 10537110]
27. Hengel RL, Thaker V, Pavlick MV, Metcalf JA, Dennis G, Yang J, et al. L-selectin (CD62L) expression distinguishes small resting memory CD4(+) T cells that preferentially respond to recall antigen. Journal of Immunology. 2003; 170(1):28–32.
28. Catron DM, Rusch LK, Hataye J, Itano AA, Jenkins MK. CD4(+) T cells that enter the draining lymph nodes after antigen injection participate in the primary response and become central-memory cells. Journal of Experimental Medicine. 2006; 203(4):1045–1054. [PubMed: 16567390]
29. Debes GF, Arnold CN, Young AJ, Krautwald S, Lipp M, Hay JB, et al. Chemokine receptor CCR7 required for T lymphocyte exit from peripheral tissues. Nature Immunology. 2005; 6(9):889–894. [PubMed: 16116468]
30. Caucheteux SM, Torabi-Parizi P, Paul WE. Analysis of naive lung CD4 T cells provides evidence of functional lung to lymph node migration. Proceedings of the National Academy of Sciences of the United States of America. 2013; 110(5):1821–1826. [PubMed: 23319636]
31. Ericsson PO, Orchansky PL, Carlow DA, Teh HS. Differential activation of phospholipase C-gamma 1 and mitogen-activated protein kinase in naive and antigen-primed CD4 T cells by the peptide/MHC ligand. Journal of Immunology. 1996; 156(6):2045–2053.
32. Kimachi K, Sugie K, Grey HM. Effector T cells have a lower ligand affinity threshold for activation than naive T cells. International Immunology. 2003; 15(7):885–892. [PubMed: 12807827]
33. London CA, Lodge MP, Abbas AK. Functional responses and costimulator dependence of memory CD4(+) T cells. Journal of Immunology. 2000; 164(1):265–272.
34. Rogers PR, Dubey C, Swain SL. Qualitative changes accompany memory T cell generation: Faster, more effective responses at lower doses of antigen. Journal of Immunology. 2000; 164(5): 2338–2346.
35. Kumar R, Ferez M, Swamy M, Arechaga I, Rejas MT, Valpuesta JM, et al. Increased Sensitivity of Antigen-Experienced T Cells through the Enrichment of Oligomeric T Cell Receptor Complexes. Immunity. 2011; 35(3):375–387. [PubMed: 21903423]
36. Anderton SM, Radu CG, Lowrey PA, Ward ES, Wraith DC. Negative selection during the peripheral immune response to antigen. Journal of Experimental Medicine. 2001; 193(1):1–11. [PubMed: 11136816]
37. Stefanova I, Dorfman JR, Germain RN. Self-recognition promotes the foreign antigen sensitivity of naive T lymphocytes. Nature. 2002; 420(6914):429–434. [PubMed: 12459785]
38. Hochweller K, Wabnitz GH, Samstag Y, Suffner J, Hammerling GJ, Garbi N. Dendritic cells control T cell tonic signaling required for responsiveness to foreign antigen. Proceedings of the National Academy of Sciences of the United States of America. 2010; 107(13):5931–5936. [PubMed: 20231464]
39. Fischer UB, Jacovetty EL, Medeiros RB, Goudy BD, Zell T, Swanson JB, et al. MHC class II deprivation impairs CD4 T cell motility and responsiveness to antigen-bearing dendritic cells in vivo. Proceedings of the National Academy of Sciences of the United States of America. 2007; 104(17):7181–7186. [PubMed: 17435166]
40. van Leeuwen EMM, Sprent J, Surh CD. Generation and maintenance of memory CD4(+) T Cells. Current Opinion in Immunology. 2009; 21(2):167–172. PMCID: PMC2676210. [PubMed: 19282163]
41. Hikono H, Kohlmeier JE, Takamura S, Wittmer ST, Roberts AD, Woodland DL. Activation phenotype, rather than central-or effector-memory phenotype, predicts the recall efficacy of memory CD8(+) T cells. Journal of Experimental Medicine. 2007; 204(7):1625–1636. [PubMed: 17606632]

42. Belz GT, Bedoui S, Kupresanin F, Carbone FR, Heath WR. Minimal activation of memory CD8+T cell by tissue-derived dendritic cells favors the stimulation of naive CD8+T cells. Nature Immunology. 2007; 8(10):1060–1066. [PubMed: 17767161]
43. Suarez-Ramirez JE, Wu T, Lee YT, Aguila CC, Bouchard KR, Cauley LS. Division of labor between subsets of lymph node dendritic cells determines the specificity of the CD8(+) T-cell recall response to influenza infection. European Journal of Immunology. 2011; 41(9):2632–2641. [PubMed: 21660939]
44. Mehlhop-Williams ER, Bevan MJ. Memory CD8(+) T cells exhibit increased antigen threshold requirements for recall proliferation. Journal of Experimental Medicine. 2014; 211(2):345–356. [PubMed: 24493801]
45. Woodworth JS, Aagaard CS, Hansen PR, Cassidy JP, Agger EM, Andersen P. Protective CD4 T Cells Targeting Cryptic Epitopes of Mycobacterium tuberculosis Resist Infection-Driven Terminal Differentiation. Journal of Immunology. 2014; 192(7):3247–3258.
46. O'Shea JJ, Paul WE. Mechanisms Underlying Lineage Commitment and Plasticity of Helper CD4(+) T Cells. Science. 2010; 327(5969):1098–1102. [PubMed: 20185720]
47. Muranski P, Restifo NP. Essentials of Th17 cell commitment and plasticity. Blood. 2013; 121(13): 2402–2414. [PubMed: 23325835]
48. Nakayamada S, Takahashi H, Kanno Y, O'Shea JJ. Helper T cell diversity and plasticity. Current Opinion in Immunology. 2012; 24(3):297–302. [PubMed: 22341735]
49. Curtis MM, Rowell E, Shafiani S, Negash A, Urdahl KB, Wilson CB, et al. Fidelity of Pathogen-Specific CD4(+) T Cells to the Th1 Lineage Is Controlled by Exogenous Cytokines, Interferon-gamma Expression, and Pathogen Lifestyle. Cell host & microbe. 2010; 8(2):163–173. [PubMed: 20709293]

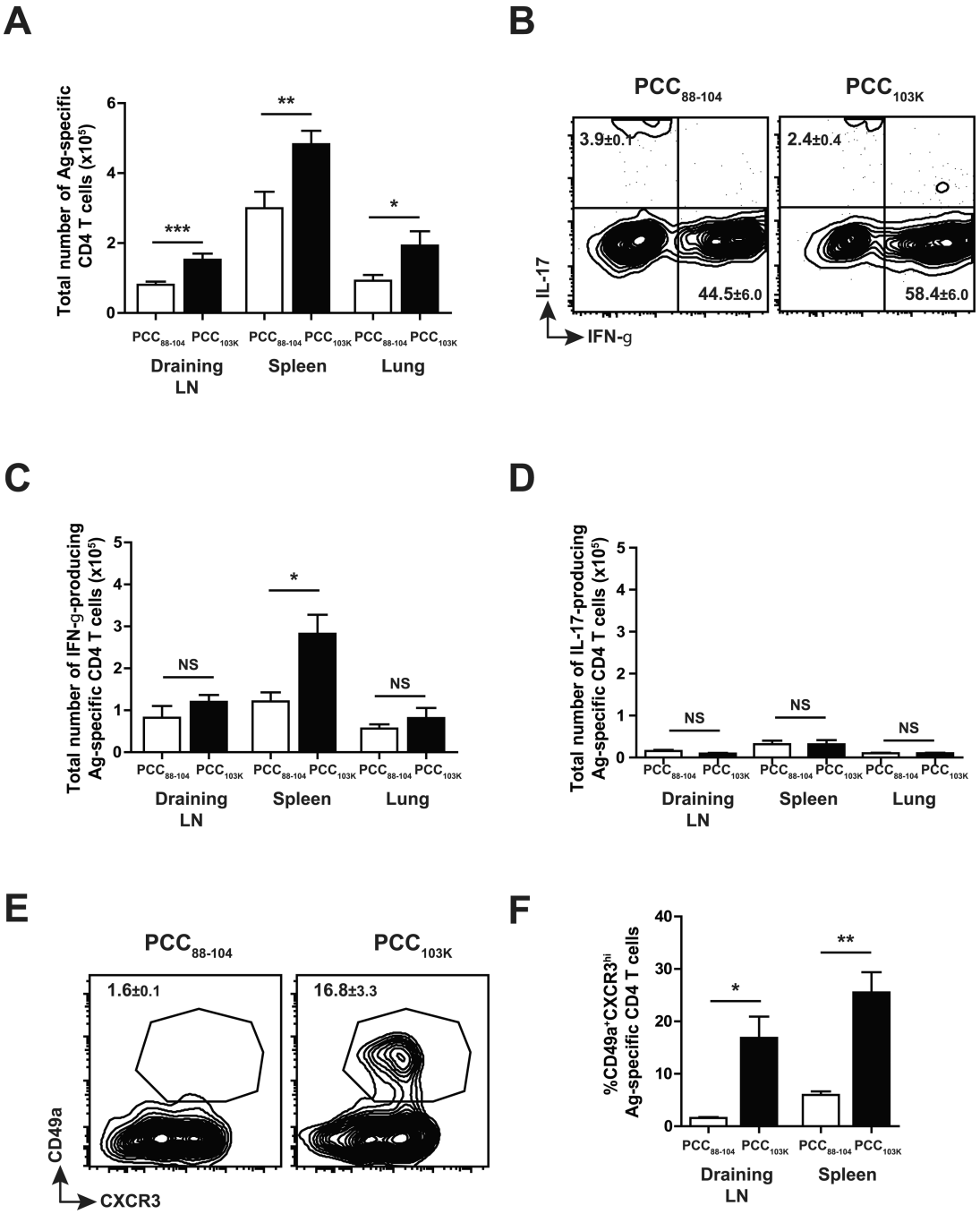

Figure 1. TCR signal strength dictates the magnitude and quality of Th1 cells

B10.BR mice were s.c. immunized with $PCC_{88–104}$ or PCC_{103K} peptides and analyzed at day 7 after immunization. (A) Total number of Ag-specific CD4 T cells ($Dapi^{-}B220^{-}CD8a^{-}CD11b^{-}V\alpha11^{+}V\beta3^{+}CD44^{hi}$). (B-D) IL-17 and IFN-γ production by Ag-specific CD4 T cells in draining LN measured by intracellular cytokine staining (ICS). Total number of IFN-γ^{+} (C) or IL-17^{+} (D) Ag-specific CD4 T cells. (E) Expression of CD49a and CXCR3 in Ag-specific CD4 T cells. (F) Frequency of $CD49a^{+}$ $CXCR3^{hi}$ Ag-specific CD4 T cells. Numbers in quadrants or above circled areas indicate percent cells (± SEM) in profile.

Means ± SEM for at least three animals are shown. *$p \leq 0.05$, **$p \leq 0.01$ (unpaired Student t test). Data shown are derived from at least three independent experiments ($n \geq 3$ mice per group).

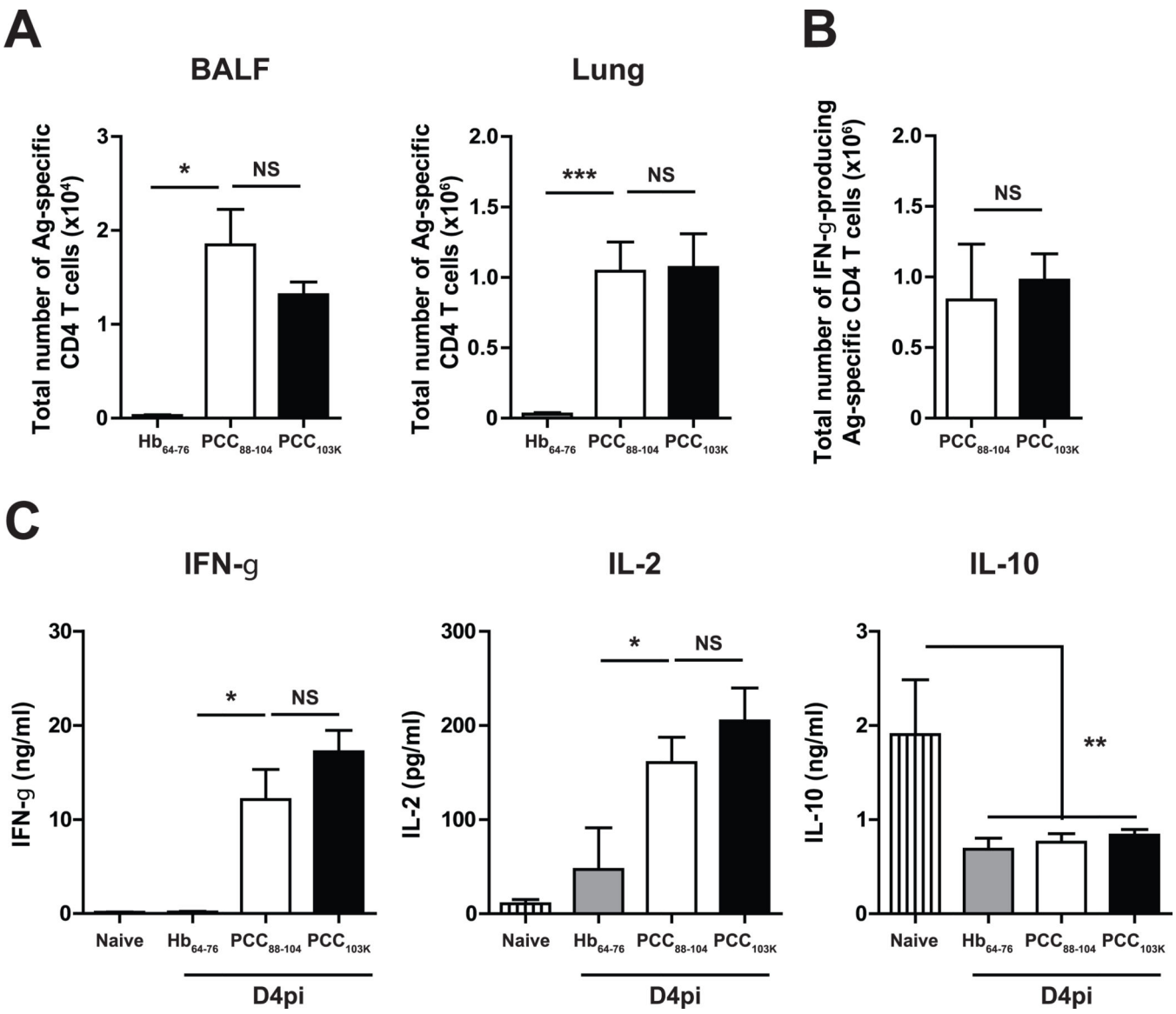

Figure 2. Rapid mobilization of effector Th1 cells during influenza infection

B10.BR mice were s.c. immunized with $Hb_{64–76}$, $PCC_{88–104}$, or PCC_{103K} peptides, challenged 7 days later with WSN-$MCC_{88–104}$ influenza virus, and analyzed on day 4 postinfection. (A) Total number of Ag-specific CD4 T cells ($Dapi^{-}B220^{-}CD8a^{-}CD11b^{-}V\alpha11^{+}V\beta3^{+}CD44^{hi}$) in BALF (left) and lungs (right). (B) Total number of IFN-γ^{+} Ag-specific CD4 T cells in lungs measured by ICS. Means ± SEM for at least three animals are shown. *$p \leq 0.05$, **$p \leq 0.01$ (unpaired Student t test). Data shown are derived from at least three independent experiments ($n \geq 3$ mice per group). (C) IL-2, IFN-γ, and IL-10 concentrations in BALF of infected ($n \geq 9$) or naïve ($n=14$) mice measured by multiplex.

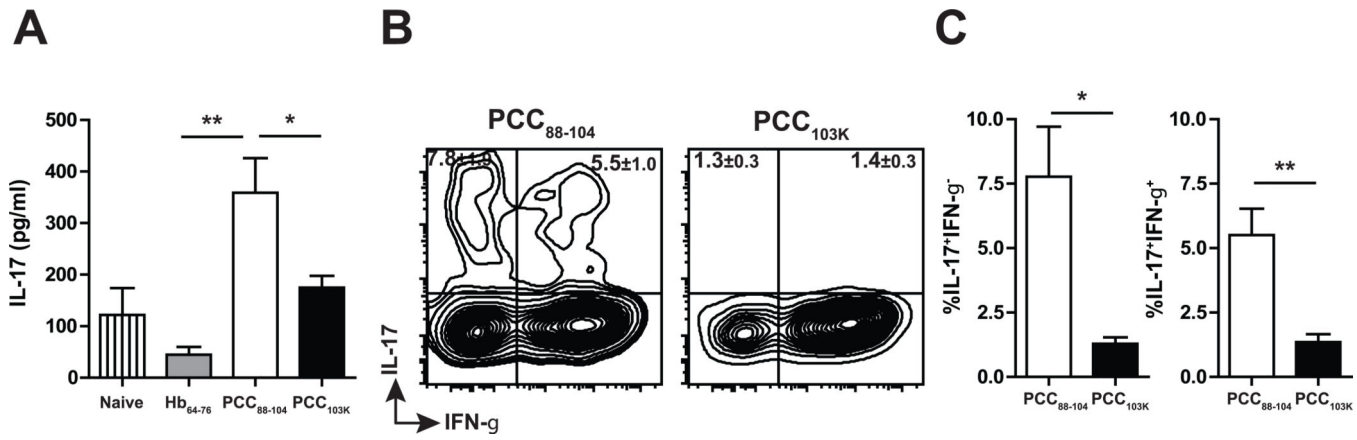

Figure 3. Th cells induced by low stability peptides produce IL-17 upon influenza infection

B10.BR mice were s.c. immunized with $Hb_{64–76}$, $PCC_{88–104}$, or PCC_{103K} peptides, challenged 7 days later with WSN-$MCC_{88–104}$ influenza virus, and analyzed on day 4 postinfection. (A) IL-17 concentration in BALF measured by multiplex. (B) IL-17 and IFN-γ production by Ag-specific CD4 T cells in draining LN measured by ICS. (C) Frequency of IL-17^+IFN-γ^- (left) or IL-17^+IFN-γ^+ (right) Ag-specific CD4 T cells measured by ICS. Numbers in quadrants indicate percent cells (± SEM) in profile. Means ± SEM for at least three animals are shown. *$p \leq 0.05$, **$p \leq 0.01$ (unpaired Student t test). Data shown are derived from at least three independent experiments ($n \geq 3$ mice per group).

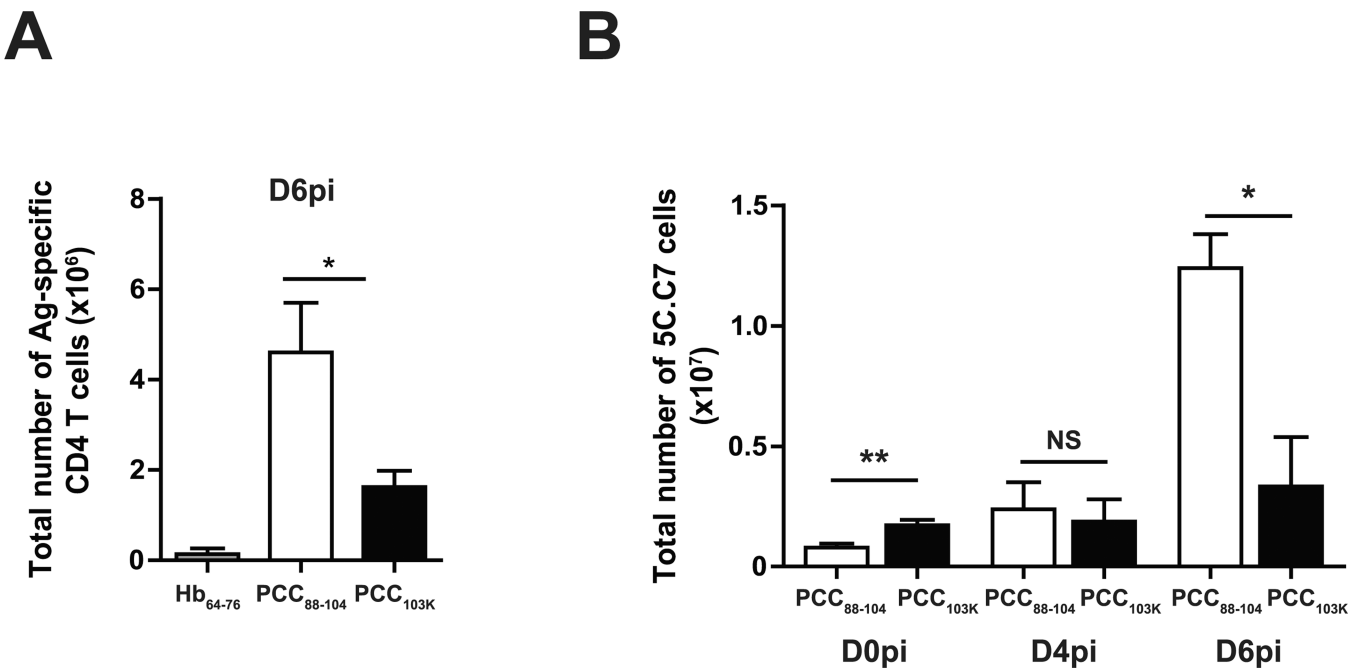

Figure 4. Better accumulation of effector CD4 T cells with low stability peptides

(A) B10.BR mice were s.c. immunized with $Hb_{64–76}$, $PCC_{88–104}$, or PCC_{103K} peptides, challenged 7 days later with WSN-$MCC_{88–104}$ influenza virus, and analyzed on day 6 after challenge. Total number of Ag-specific CD4 T cells ($Dapi^{-}B220^{-}CD8a^{-}CD11b^{-}V\alpha11^{+}V\beta3^{+}CD44^{hi}$) in lung. (B) Splenocytes from $Thy1.2^{+}$ 5C.C7αβ TCR transgenic mice were adoptively transferred into congenic $Thy1.1^{+}$ mice. Recipient mice were s.c. immunized with $PCC_{88–104}$ or PCC_{103K} peptides and challenged 7 days later with WSN-$MCC_{88–104}$ influenza virus. Total number of 5C.C7 cells ($Dapi^{-}B220^{-}CD8a^{-}CD11b^{-}Thy1.2^{+}CD44^{hi}$) in lungs on days 0, 4, and 6 postinfection. Means ± SEM for at least three animals are shown. *$p \leq 0.05$, **$p \leq 0.01$ (unpaired Student t test). Data shown are derived from at least three independent experiments ($n \geq 3$ mice per group).

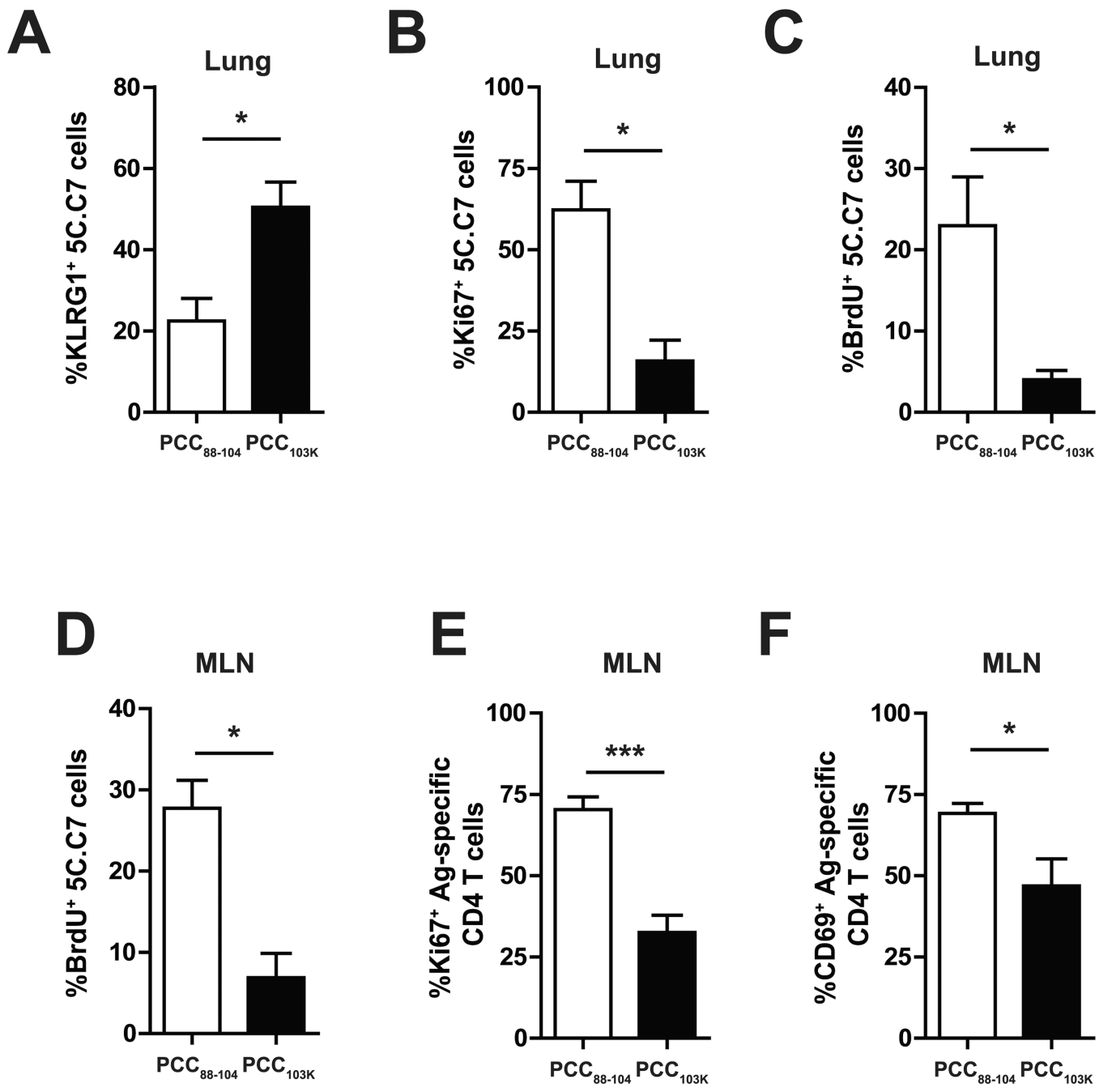

Figure 5. Dampened proliferative recall response in mice primed with strong TCR signaling

(A–D) Splenocytes from 5C.C7αβ TCR transgenic mice were adoptively transferred into congenic mice. The recipient mice were s.c. immunized with $PCC_{88–104}$ or PCC_{103K} peptides, challenged 7 days later with WSN-$MCC_{88–104}$ influenza virus, and analyzed on day 4 postinfection. (A–C) Frequency of $KLRG1^+$ (A), $Ki67^+$ (B), or $BrdU^+$ (C) 5C.C7 cells in lung. (D) Frequency of $BrdU^+$ 5C.C7 cells in MLN. (E–F) B10.BR mice were s.c. immunized with $PCC_{88–104}$ or PCC_{103K} peptides. After 7 days, mice were infected with WSN-$MCC_{88–104}$ influenza virus and analyzed on day 4 postinfection. Frequency of $Ki67^+$ (E) or $CD69^+$ (F) Ag-specific CD4 T cells ($Dapi^-B220^-CD8a^-CD11b^-V\alpha11^+V\beta3^+CD44^{hi}$)

in MLN. Means ± SEM for at least three animals are shown. *$p \leq 0.05$, **$p \leq 0.01$, ***$p \leq 0.001$ (unpaired Student t test). Data shown are derived from at least three independent experiments ($n \geq 3$ mice per group).

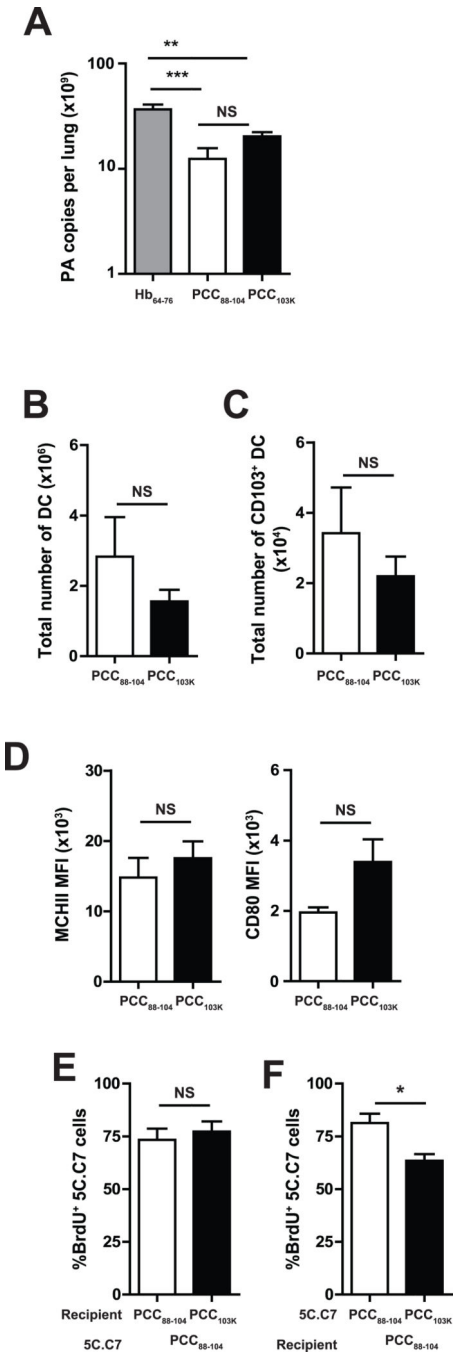

Figure 6. Defective proliferation of high stability peptides-primed Th cells is T cell intrinsic

(A–D) B10.BR mice were s.c. immunized with $PCC_{88–104}$ or PCC_{103K} peptides. After 7 days, mice were infected with WSN-$MCC_{88–104}$ influenza virus. (A) At day 4 postinfection, mice were sacrificed, lungs were removed, RNA was isolated, and quantitative PCR was performed as described in Materials and Methods. PA copy number per lung is shown for six mice per group. (B–D) At day 2 postinfection, mice were sacrificed and MLNs were removed. (B–sC) Total number of (B) DCs (defined as $CD3^{-}CD19^{-}DAPI^{-}MHCII^{+}CD11c^{+}$ cells) or (C) $CD103^{+}$ DCs in MLN. (D) MFI of MHCII and CD80 in $CD103^{+}$ DC in MLN.

(E–F) Splenocytes from 5C.C7αβ TCR transgenic mice were adoptively transferred into congenic mice and recipient mice were s.c. immunized with $PCC_{88–104}$ or PCC_{103K} peptides. After 7 days, 5C.C7 cells were sorted and transferred to secondary recipients immunized with $PCC_{88–104}$ or PCC_{103K} peptides 7 days before. Secondary recipients were infected with WSN-$MCC_{88–104}$ influenza virus and analyzed on day 4 postinfection. (E) Frequency of $BrdU^+$ among $PCC_{88–104}^-$primed 5C.C7 cells in $PCC_{88–104}^-$ or PCC_{103K}-immunized recipients. (F) Frequency of $BrdU^+$ among $PCC_{88–104}^-$ or PCC_{103K}-primed 5C.C7 in $PCC_{88–104}^-$immunized recipients. Means ± SEM for at least three animals are shown. *$p \leq 0.05$ (unpaired Student t test). Data shown are derived from at least three independent experiments ($n \geq 3$ mice per group).

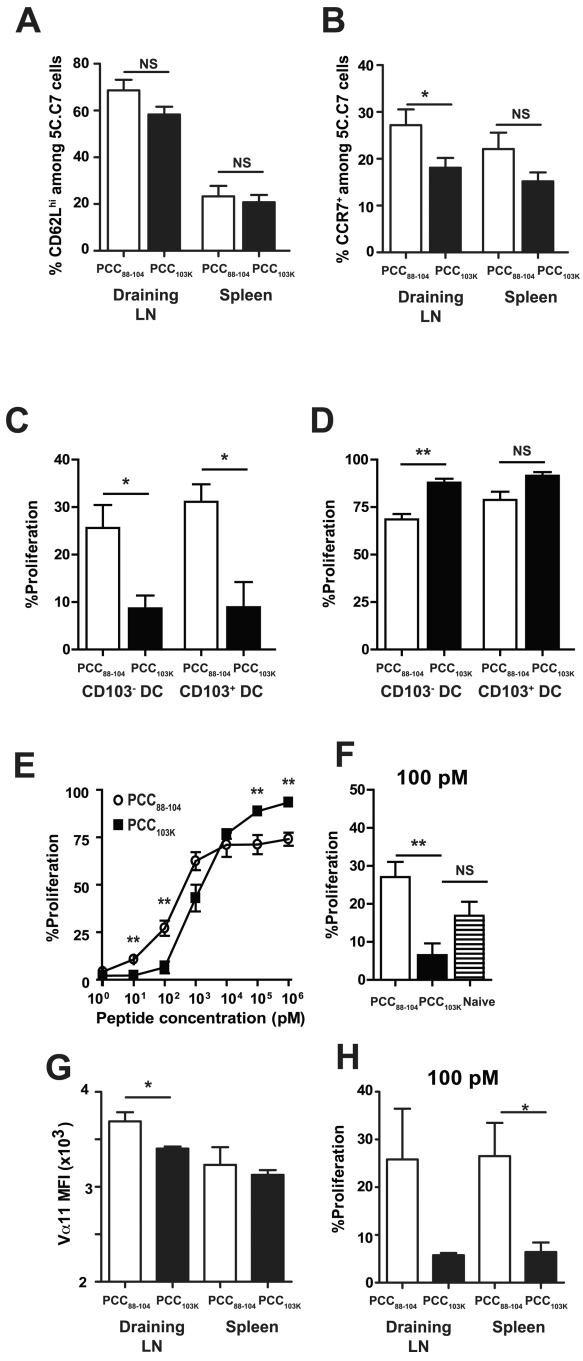

Figure 7. High stability peptide-induced Th cells fail to proliferate in response to lung DCs from infected mice

Splenocytes from 5C.C7αβ TCR transgenic mice were adoptively transferred into congenic mice, and recipient mice were s.c. immunized with $PCC_{88–104}$ or PCC_{103K} peptides. (A) Frequency of $CD62L^{hi}$ or (B) $CCR7^{+}$ 5C.C7 cells in the indicated organs 7 days after immunization with indicated peptides. Means ± SEM for at least six animals are shown. (C-F) Draining LN and spleen of recipient mice were harvested 7 days after immunization. 5C.C7 cells were sorted and CFSE-labeled. (C–D) CFSE-labeled 5C.C7 day 7 effector cells were cultured without (C) or with (D) 1 μM $MCC_{88–103}$ peptide and $CD103^{+}$ or $CD103^{–}$

DCs sorted from MLNs of B10.BR mice infected with WSN-$MCC_{88–104}$ influenza virus 2 days before. (E–F) CFSE-labeled 5C.C7 day 7 effector cells and (F) naïve 5C.C7 cells were cultured with purified splenic DCs from naïve mice and (E) various concentrations of $MCC_{88–103}$ peptide or (F) 100 pM of $MCC_{88–103}$ peptide. After 72 h, cell division was determined by flow cytometry. Frequencies of dividing CD4 T cells ($Thy1.2^{+}CFSE^{lo}$) are displayed. (G) Vα11 staining MFI of 5C.C7 cells in indicated organs 7 days after immunization. (H) CFSE-labeled 5C.C7 day 7 effector cells derived from draining LN or spleen were cultured with purified splenic DCs from naïve mice and 100 pM of $MCC_{88–103}$ peptide. After 72 h, cell division was determined by flow cytometry. Frequencies of dividing CD4 T cells (Thy1.2+CFSElo) are displayed. Means ± SEM for at least three animals are shown. *$p \leq 0.05$, (unpaired Student t test), **$p \leq 0.01$ (unpaired Student t test). Data shown are derived from at least three independent experiments ($n \geq 3$ mice per group).